analysis of a waveguide mounting structure," *IEEE Trans. Microwave Theory Tech.*, vol. MTT-19, pp. 706–719, Aug. 1971.
[25] R. P. Owens and D. Cawsey, "Microwave equivalent circuit parameter of Gunn effect devices packages," *IEEE Trans. Microwave Theory Tech.*, vol. MTT-18, pp. 780–798, 1970.
[26] K. Wilson, "Gunn effect devices and their applications," *Mullard Techn. Comm.* vol. 10, pp. 286–293, 1969.
[27] A. A. Sweet and L. A. MacKenzie, "The FM noise of a C.W. Gunn oscillator," *Proc. IEEE* vol. 58, pp. 822–823, 1970.
[28] O. L. El-Sayed, "Generalized analysis of parallel two-post mounting structures in waveguide," *IEEE Trans. Microwave Theory Tech.*, vol. MTT-25, pp. 24–33, 1977.
[29] J. S. Joshi and A. F. Cornick, "Analysis of waveguide post configurations: part I—Gap admittance matrices," *IEEE Trans. Microwave Theory Tech.*, vol. MTT-25, pp. 169–173, Mar. 1977.
[30] ——, "Analysis of waveguide post configuration: part II—Dual gap cases," *IEEE Trans. Microwave Theory Tech.*, vol. MTT-25, pp. 173–181, Mar. 1977.
[31] K. Talwar, W. R. Curtice, "Effect of donor density and temperature on the performance of stabilized transferred-electron devices," *IEEE Trans. Electron. Devices*, vol. ED-20, pp. 544–550, June 1973.
[32] G. S. Hobson and B. A. E. DeSa, "Thermal effects in the bias circuit frequency modulation of Gunn oscillators," *IEEE Trans. Electron. Devices*, vol. ED-18, pp. 557–562, 1971.
[33] R. Stevens and F. A. Myers, "Temperature compensation of Gunn oscillator," *Electron. Lett.*, vol. 10, pp. 461–463, 1974.
[34] A. Kondo, T. Ishii and K. Shirata, "Simple stabilizing method for solid state microwave oscillators," *IEEE Trans. Microwave Theory Tech.*, vol. MTT-22, pp. 970–972, Nov. 1974.

Theory and Simulation of the Gyrotron Traveling Wave Amplifier Operating at Cyclotron Harmonics

KWO RAY CHU, ADAM T. DROBOT, HAROLD HWALING SZU, and PHILLIP SPRANGLE

***Abstract*—An analytical expression for the efficiency of the gyrotron traveling wave amplifier is derived for the case of nonfundamental cyclotron harmonic interaction. It scales the efficiency with respect to the modes and parameters of operation. This relation, together with a general linear dispersion relation, also derived in the present paper, gives the characteristics and optimum operation conditions of the gyrotron traveling wave amplifier.**

I. Introduction

AN INTERESTING electromagnetic radiation mechanism [1]–[3] known as the electron cyclotron maser has been the subject of intense research activities in recent years. This mechanism has been the basis for a new class of microwave devices called gyrotrons capable of generating microwaves at unprecedented power levels at millimeter and submillimeter wavelengths. A detailed description of the cyclotron maser mechanism is given in [4] and brief summaries of gyrotron theories and experiments, together with lists of references, can be found in recent review papers [5]–[7].

In the present study, we will concentrate on a particular type of gyrotrons—the gyrotron traveling wave amplifier (gyro-TWA). The cyclotron maser instability and its wide-band amplification capability was demonstrated experimentally by Granatstein *et al.* [8] on an intense relativistic electron beam. The basic physical processes taking place in a gyro-TWA have been analyzed in recent linear and nonlinear theories [4],[9]–[16]. In the actual operation of a gyro-TWA, the beam-to-wave energy conversion efficiency is one of the most important considerations. References [12]–[14] contain detailed studies of the saturation mechanisms and calculations of efficiency for the operation at the fundamental cyclotron harmonic. However, the scaling of the efficiency with respect to the various modes and parameters of operation has not been considered in any detail, nor has the operation at the nonfundamental cyclotron harmonics. The nonfundamental harmonic operation is of great importance for the amplification of submillimeter waves if unrealistically high magnetic fields (>100 kG) are to be avoided. In anticipation of the growing experimental effort aimed at the generation of submillimeter waves, our main purpose in the present study is to derive a general analytical expression for the operating efficiency.

Manuscript received May 30, 1979; revised November 26, 1979. This work was supported by Rome Air Development Center under MIPR FY761970026.

K. R. Chu, H. H. Szu, and P. Sprangle are with the Naval Research Laboratory, Washington, DC 20375.
A. T. Drobot is with Science Applications, Inc., McLean, VA 22101.

II. Derivation of a General Dispersion Relation

The typical configuration of a gyro-TWA consists of an annular electron beam propagating inside a waveguide of

0018-9480/80/0400-0313$00.75 ©1980 IEEE

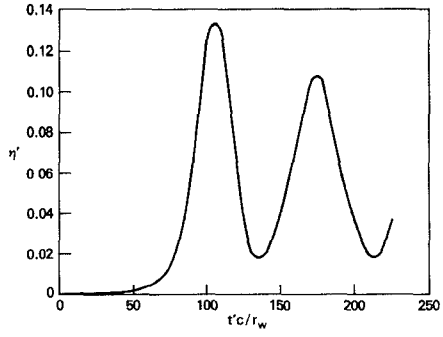

Fig. 1. Cross-sectional view of the gyro-TWA model. The applied magnetic field (not shown) points toward the reader. The electrons are monoenergetic and all have the same Larmor radius r_L. Guiding centers of all electrons are uniformly distributed on the circle of constant radius r_0.

circular cross section of radius r_w (Fig. 1). The electrons, guided by a uniform magnetic field ($B_0 e_z$), move along helical trajectories. In our model, we assume that the beam is sufficiently tenuous that its space charge electric field can be neglected, and the spatial structure of the vacuum waveguide mode is unaffected by the presence of the beam. The beam interacts with a single TE_{mn} waveguide mode, where m and n are, respectively, the azimuthal and radial eigenmode numbers. The dynamics of the electron beam is described by the linearized relativistic Vlasov equation

$$\left(\frac{\partial}{\partial t}+v\cdot\frac{\partial}{\partial x}-ev\times B_0 e_z\cdot\frac{\partial}{\partial p}\right)f^{(1)} = e(E^{(1)}+v\times B^{(1)})\cdot\frac{\partial}{\partial p}f_0 \quad (1)$$

where f_0 and $f^{(1)}$ are the initial and perturbed distribution functions, respectively, and $E^{(1)}, B^{(1)}$ are the wave fields of the TE_{mn} waveguide mode, i.e.,

$$B_z^{(1)}=\hat{B}_z J_m(\alpha_{mn}r)\mathrm{Re}[\exp(im\theta+ik_z z-i\omega t)]$$

$$B_r^{(1)}=\hat{B}_z k_z(2\alpha_{mn})^{-1}[J_{m-1}(\alpha_{mn}r)-J_{m+1}(\alpha_{mn}r)]\cdot\mathrm{Re}[i\exp(im\theta+ik_z z-i\omega t)]$$

$$B_\theta^{(1)}=-\hat{B}_z k_z(2\alpha_{mn})^{-1}[J_{m-1}(\alpha_{mn}r)+J_{m+1}(\alpha_{mn}r)]\cdot\mathrm{Re}[\exp(im\theta+ik_z z-i\omega t)]$$

$$E_r^{(1)}=\omega B_\theta^{(1)}/k_z c$$

$$E_\theta^{(1)}=-\omega B_r^{(1)}/k_z c$$

where $\hat{B}_z$ is the amplitude of the wave magnetic field, $\alpha_{mn}\equiv x_{mn}/r_w$, x_{mn} is the nth root of $J_m'(x)=0$, J_m is the Bessel function of order m, and $J_m'(x)=dJ_m(x)/dx$. Note that the validity of the linear theory requires $B_z\ll B_0$ and $f^{(1)}\ll f_0$. From (1) and the Maxwell equations, we obtain

$$(\omega^2/c^2-k_z^2-\alpha_{mn}^2)\hat{B}_z J_m(\alpha_{mn}r) = -\frac{4\pi}{c}\exp(-im\theta-ik_z z+i\omega t)\frac{1}{r}\left[\frac{\partial}{\partial r}(rJ_\theta^{(1)})-imJ_r^{(1)}\right] \quad (2)$$

where $J_{\theta r}^{(1)}$ is the perturbed beam current given by

$$J_{\theta,r}^{(1)}=-e\int f^{(1)}v_{\theta,r}\,d^3p. \quad (3)$$

Multiplying (2) by $rJ_m(\alpha_{mn}r)$ and integrating over r from 0 to r_w, we obtain

$$\frac{\omega^2}{c^2}-k_z^2-\alpha_{mn}^2=\frac{8\pi\alpha_{mn}\exp(-im\theta-ik_z z+i\omega t)}{cr_w^2K_{mn}\hat{B}_z}\cdot\int_0^{r_w}dr\left[-rJ_\theta^{(1)}J_{m+1}(\alpha_{mn}r)+\frac{m}{\alpha_{mn}}J_\theta^{(1)}J_m(\alpha_{mn}r)+\frac{im}{\alpha_{mn}}J_r^{(1)}J_m(\alpha_{mn}r)\right] \quad (4)$$

where

$$K_{mn}=J_m^2(x_{mn})[1-m^2/x_{mn}^2].$$

Equations (1) through (4) form a complete set of equations. To solve these equations, one must first specify the form of the initial electron distribution function in terms of the constants of motion of the system, namely, the perpendicular and parallel momenta $p_\perp$ and p_z, and the canonical angular momentum P_θ. To be consistent with the experimental configuration that all the electron guiding centers are located on the same cylindrical surface defined by $r=r_0$ (see Fig. 1), we choose f_0 to be of the form

$$f_0=K\delta(r_L^2-2P_\theta/eB_0-r_0^2)g(p_\perp,p_z) \quad (5)$$

where $\delta(x)$ is the Dirac delta function, $r_L=p_\perp/eB_0$ is the electron Larmor radius, $g(p_\perp,p_z)$ is an arbitrary function of $p_\perp$ and p_z satisfying $\int g\,d^3p=1$, and K is a normalization constant chosen to satisfy $\int f_0 2\pi r dr d^3p=N$, where N is the number of electrons per unit axial length. To derive the dispersion relation from these equations, we first solve for $f^{(1)}$ from (1), then insert $f^{(1)}$ into (3) to calculate $J_\theta^{(1)}$ and $J_r^{(1)}$. The final expression for the dispersion relation is then obtained by substituting $J_{\theta,r}^{(1)}$ into (4) and carrying out the r integration. Considerable algebra is involved in this integration; however, the procedures are straightforward and standard. Here we present the result directly,

$$\frac{\omega^2}{c^2}-k_z^2-\alpha_{mn}^2=\frac{-8\pi\nu}{r_w^2K_{mn}}\int_0^\infty p_\perp dp_\perp\int_{-\infty}^\infty dp_z g(p_\perp,p_z)\cdot\left[\frac{(\omega^2-k_z^2c^2)p_\perp^2H_{Sm}(\alpha_{mn}r_0,\alpha_{mn}r_L)}{\gamma^3m^2c^2(\omega-k_z v_z-s\Omega_c)^2}-\frac{(\omega-k_z v_z)Q_{Sm}(\alpha_{mn}r_0,\alpha_{mn}r_L)}{\gamma(\omega-k_z v_z-s\Omega_c)}\right] \quad (6)$$

where

$$\Omega_c=eB_0/\gamma m$$

$$\gamma=[1+(p_\perp^2+p_z^2)/m^2c^2]^{1/2}$$

$$\nu=Nr_e$$

$$r_e=\mu_0e^2/4\pi m=2.8\times10^{-12}\ \mathrm{cm}$$

is the classical electron radius. The functions H_{sm} and Q_{sm} are defined as follows:

$$H_{sm}(x,y)=\left[J_{s-m}(x)J_s'(y)\right]^2$$

$$Q_{sm}(x,y)=2H_{sm}(x,y)+y\left[J_{s-m}^2(x)J_s'(y)J_s''(y)\right.$$

$$\left.+\tfrac{1}{2}J_{s-m-1}^2(x)J_s'(y)J_{s-1}'(y)-\tfrac{1}{2}J_{s-m+1}^2(x)J_s'(y)J_{s+1}'(y)\right].$$

The dispersion relation in (6) is very general in that the waveguide mode numbers m, n, and the cyclotron harmonic number s are all treated as free parameters. This will provide the option to analyze all possible interactions as one searches for the optimum efficiency. Furthermore, thermal effect is also included in (6). One can investigate the thermal effect by specifying a momentum space distribution function $g(p_\perp,p_z)$ appropriate for the beam used and carrying out the $p_\perp$ and p_z integrations. For the present study, however, we will concentrate on an idealized cold electron beam represented by the following distribution function:

$$g(p_\perp,p_z)=(2\pi p_\perp)^{-1}\delta(p_\perp-p_{\perp 0})\delta(p_z-p_{z0}). \quad (7)$$

Substituting (7) into (6) and carrying out the $p_\perp$ and p_z integrations, we obtain the dispersion relation for a cold beam,

$$\frac{\omega^2}{c^2}-k_z^2-x_{mn}^2/r_w^2=\frac{-4\nu}{\gamma_0 r_w^2 K_{mn}}\cdot\left[\frac{(\omega^2-k_z^2c^2)\beta_{\perp 0}^2 H_{sm}(x_{mn}r_0/r_w,x_{mn}r_{L0}/r_w)}{(\omega-k_zv_{z0}-s\Omega_c)^2}\right.$$

$$\left.-\frac{(\omega-k_zv_{z0})Q_{sm}(x_{mn}r_0/r_w,x_{mn}r_{L0}/r_w)}{\omega-k_zv_{z0}-s\Omega_c}\right] \quad (8)$$

where

$$\gamma_0=\left[1+(p_{\perp 0}^2+p_{z0}^2)/m^2c^2\right]^{1/2}$$

$$v_{\perp 0}=p_{\perp 0}/\gamma_0 m$$

$$v_{z0}=p_{z0}/\gamma_0 m$$

$$\beta_{\perp 0}=v_{\perp 0}/c$$

$$r_{L0}=v_{\perp 0}/\Omega_c.$$

On the right-hand side of (8), the first term is the source of the instability, while the second term imposes a threshold beam energy for the instability. For the nonfundamental harmonics ($s>1$), it can be shown that the threshold energy (typically below 1 keV) is much lower than the typical beam energy (tens of kilo electron volts); hence the second term can be neglected. Substituting $\omega=\omega_0+\Delta\omega, k_z=k_{z0}$ into (8), where (ω_0,k_{z0}) is the point at which the waveguide characteristic curve

$$\omega^2-k_z^2c^2-x_{mn}^2c^2/r_w^2=0 \quad (9)$$

intersects with the beam characteristic curve

$$\omega-k_zv_{z0}-s\Omega_c=0 \quad (10)$$

we can easily evaluate $\Delta\omega(=\Delta\omega_r+i\Delta\omega_i)$, with the result

$$\Delta\omega_r=\left[\frac{\nu x_{mn}^2 H_{sm}\beta_{\perp 0}^2 c^4}{4\gamma_0 K_{mn}\omega_0 r_w^4}\right]^{1/3} \qquad \Delta\omega_i=\sqrt{3}\,\Delta\omega_r. \quad (11)$$

In (11), $\Delta\omega_r$ gives the frequency width for resonant beam-wave interaction, and $\Delta\omega_i$ gives the growth rate.

III. Numerical Simulations

The preceding linear analysis has been complemented by a single-wave numerical simulation code [16] developed to simulate the amplification of the TE_{0n} mode at an arbitrary cyclotron harmonic frequency. Fig. 2 shows a typical efficiency curve as a function of time. It exponentiates at twice the linear growth rate, then exhibits an oscillatatory behavior after saturation. We add in passing that such oscillatory behavior has been observed in a recent experiment [17]. The simulation shows two different but simultaneously present saturation mechanisms—depletion of free electron energy and loss of phase synchronism. The first mechanism dominates when the beam energy is slightly above threshold. Saturation occurs as soon as the beam loses a small amount of energy and the system becomes linearly stable. The second mechanism dominates when the beam energy is well above the threshold. Saturation occurs because an average electron loses so much energy that its relativistic cyclotron frequency no longer matches the wave frequency to favor unstable interactions. As found in [13], both mechanisms are important for the fundamental cyclotron harmonic interaction. However, there is a basic difference between the fundamental and nonfundamental harmonic interactions; namely, for the latter interaction, we find that the threshold beam energy is typically so low that the energy depletion saturation mechanism can be disregarded. This has allowed us to derive below an analytical scaling relation for the efficiency.

IV. Efficiency Scaling Relation

For the purpose of efficiency optimization in the multiple parameter space typical of gyro-TWA system, an analytical scaling relation would be most useful. For generality, we shall derive the efficiency scaling relation in the beam reference frame (i.e., the frame in which $v_{z0}=0$), and denote the beam frame quantities with a prime. A simple Lorentz transformation [14] can be used to convert the beam frame efficiency into lab frame efficiency. In order to minimize the possibility of spurious oscillations, it is advantageous to choose a magnetic field such that (9) and (10) intersect at only one point (i.e., at a grazing angle). In the beam frame, this implies

$$\omega_0'=s\Omega_c'=x_{mn}c/r_w. \quad (12)$$

Henceforth, our analysis will be restricted to this particular case.

In the linear analysis, we have shown that the following condition holds at the onset of the instability,

$$\omega_r'-s\Omega_e/\gamma_0'=\Delta\omega_r' \quad (13)$$

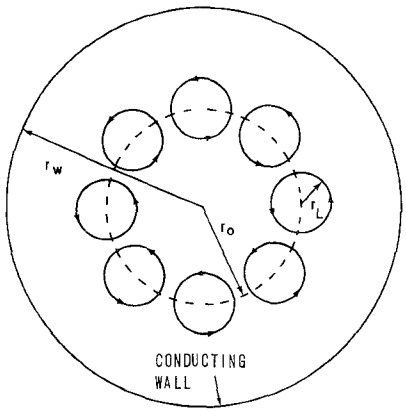

Fig. 2. Simulated efficiency versus time for $m=0$, $n=s=2$, $\nu'=0.002$, $\gamma_0'=1.1$, and $r_0/r_w=0.44$.

where $\Omega_e=eB_0/m$ and $\Delta\omega_r'$ is a positive quantity given by (11). As the instability evolves, the average energy of the electrons decreases, hence the left-hand side of (13) also decreases. Knowing this tendency and the width for resonant interaction, we expect the following condition to hold at the saturation state,

$$\omega_r'-s\Omega_e/\langle\gamma_s'\rangle\cong-\Delta\omega_r' \tag{14}$$

where $\langle\gamma_s'\rangle$ is the average γ' of all the electrons at saturation. This is the physically expected saturation condition because any further decrease in electron energy would shift the electron cyclotron frequency out of the range for resonant beam-wave interaction. Equation (14) was found to be in good agreement with our extensive simulation data.

From (12) to (14) and assuming $\gamma_0'-\langle\gamma_s'\rangle\ll\gamma_0'$, we obtain an approximate estimate for the efficiency η',

$$\eta'=\frac{\gamma_0'-\langle\gamma_s'\rangle}{\gamma_0'-1}\cong\frac{2\gamma_0'\Delta\omega_r'}{(\gamma_0'-1)\omega_0'}. \tag{15}$$

To compare (15) with the simulation data, we note that the efficiency does not asymptote to a constant value in the simulation runs. Rather, it oscillates in the large signal regime (Fig. 2). Equation (15) is found to be in very good agreement with the simulation data for nonfundamental cyclotron harmonics in the sense that it consistently predicts an efficiency at approximately 75–80 percent of the simulated *peak* value. Thus in order to scale the peak efficiency, we multiply the right hand side of (15) by 1.25. After substitution of (11), (12) for $\Delta\omega_r$ and ω_0' we obtain

$$\eta'=\frac{1.25}{\gamma_0'-1}\left[\frac{2\nu'\gamma'^2H_{sm}(x_{mn}r_0/r_w x_{mn}r_{L0}/r_w)\beta_{\perp 0}'^2}{K_{mn}x_{mn}^2}\right]^{1/3} \tag{16}$$

where H_{sm}, K_{mn}, and x_{mn}, r_0, and r_w are all frame independent quantities.

Equation (16) shows how η' scales with the mode numbers m, n, s, and the operating parameters ν', γ_0', and r_0. Note that η' is independent of the waveguide radius r_w. The scaling of η' with respect to ν' is especially simple;

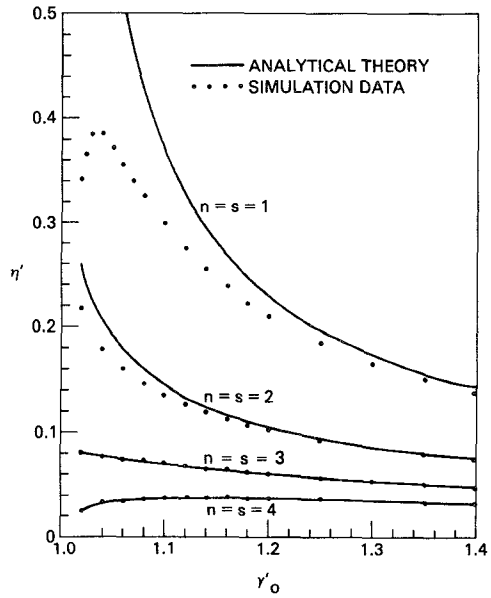

Fig. 3. Efficiency versus beam energy for $m=0$, $\nu'=0.002$, and optimized values of $r_0(r_0/r_w=0.48$, 0.44, 0.41, and 0.40 for $n=s=1,2,3,4$, respectively). Solid curves are obtained from (16) and dots are simulation data.

namely, $\eta\propto\nu'^{1/3}$. This scaling relation is valid to the extent that the tenuous beam assumption made preceding (1) is valid. In most gyrotron experiments, the beam power ranges from tens to hundreds of kilowatts and the tenuous beam assumption is easily justified. For a given mode of operation, the choice of r_0 should be such that H_{sm} falls on or near its peak value. Scaling of η' with respect to m, n, s, and γ_0 is more complicated and can best be seen through numerical plots of (16). Some examples are shown in Fig. 3, in which η' is plotted (solid curves) against the beam energy (γ_0') for $m=0$, $\nu'=0.002$, $s=n=1$, 2, 3, and 4. In each case, the beam position (r_0) has been chosen to maximize H_{sm}; namely, we have chosen $r_0/r_w=0.48$, 0.44, 0.41, and 0.40 for $s=n=1$, 2, 3, and 4, respectively. For comparison, the numerical simulation data (e.g., the peak efficiency of Fig. 2) were also shown on the same figure (dots). Equation (16) was derived by neglecting the energy depletion mechanism, which is important for the fundamental cyclotron harmonic at low beam energies. This explains the disagreement between (16) and the simulation data in the case of the fundamental cyclotron harmonic ($s=1$). For this case, only the simulation data on Fig. 3 is relevant, while the analytic curve was plotted to illustrate the inapplicability of (16) to the fundamental cyclotron harmonic interaction. For the second cyclotron harmonic ($s=2$), the agreement between (16) and the simulation data is generally good except for the small discrepancy at low beam energies. This discrepancy is due to the fact that the energy depletion saturation mechanism still plays a minor role at low beam energies. For the third and higher cyclotron harmonics, (16) is in excellent agreement with the simulation data for all beam energies. One observes

from Fig. 3 that higher cyclotron harmonics generally give lower efficiency as expected and the behavior of efficiency as a function of the beam energy is different for different cyclotron harmonics. Finally, we note that the results shown in Fig. 3 are obtained for a magnetic field (12) which maximizes the bandwidth instead of the efficiency. As shown in [14] and [16], the efficiency can be significantly enhanced at the cost of lower (small signal) gain and bandwidth by slightly lowering the magnetic field.

To convert the beam reference frame quantities in (16) into the lab frame, we need to specify the beam axial velocity v_{z0} as observed in the lab frame. Defining

$$\gamma_z = (1-\beta_{z0}^2)^{-1/2} \tag{17}$$

where $\beta_{z0} = v_{z0}/c$, we can write the conversion formulas as

$$\eta = \gamma_z(\gamma_0'-1)\eta'/(\gamma_z\gamma_0'-1) \tag{18}$$

$$\nu = \gamma_z \nu' \tag{19}$$

$$\gamma_0 = \gamma_z \gamma_0' \tag{20}$$

$$\beta_{\perp 0} = \beta_{\perp 0}'/\gamma_z \tag{21}$$

$$g = 8.7\omega_i/v_{z0} \text{ dB/unit length} \tag{22}$$

$$I_b = 1.707\times 10^4 \nu \beta_{z0} \text{ A.} \tag{23}$$

As an example, we consider the electron beam used in Fig. 3 (i.e., $\gamma_0' = 1.1$ and $\nu' = 0.002$). We specify that the beam moves at a velocity $v_{z0} = 0.266c$ in the laboratory frame, hence $\gamma_z = 1.037$. Applying (18)–(23), we obtain $\eta = 0.73\eta'$, $\nu = 2.07\times 10^{-3}$, $\gamma_0 = 1.14$ (i.e, beam voltage$\approx$ 70 kV), $g = 1.09\times 10^{-9}\omega_i$ dB/cm, and $I_b = 9.4$ A, where η' is to be calculated from (16) and ω_i (in s^{-1}) from (8) or (11) after other parameters ($m, n, s, \Omega_c, r_0, r_w$, etc.) are also specified.

To summarize, we presented a general linear dispersion relation and a concise efficiency scaling relation for the gyro-TWA. These results represent the first comprehensive analytical and simulation studies of the nonfundamental harmonic interactions. The linear dispersion relation, (6) or (8), is applicable to the fundamental as well as nonfundamental cyclotron harmonics and can be used to calculate the small signal gain, the bandwidth, and the effect due to beam velocity spread, etc. The efficiency scaling relation (16) gives a fairly accurate estimate of the efficiency for the nonfundamental cyclotron harmonics. For application to experiments, the two relations combined provide an analytical basis for assessing the feasibility of a given experimental goal and for selecting the optimum mode and parameters to achieve it. Experimental investigations of the gyro-TWA are being carried out at the Naval Research Laboratory [17] and Varian Associates [18]. Preliminary results are found to be in good agreement with the present theory.

ACKNOWLEDGMENT

The authors are grateful to many discussions held with Dr. S. Ahn, Dr. M. Baird, Dr. L. Barnett, Dr. V. Granatstein, Dr. H. Jory, Dr. M. Read, Dr. R. Symons, and Dr. H. Uhm.

REFERENCES

[1] R. Q. Twiss, "Radiation transfer and the possibility of negative absorption in radio astronomy," *Austrian J. Phys.* vol. 11, pp. 564–579, 1958.

[2] J. Schneider, "Stimulated emission of radiation by relativistic electrons in magnetic field," *Phys. Rev. Lett.* vol. 2, pp. 504–505, 1959.

[3] A. V. Gaponov, "Interaction between electron fluxes and electromagnetic waves in waveguides." *Izv. VUZ., Radiofiz.* vol. 2, pp. 450–462, 1959 and "Addendum," *Izv. VUZ., Radiofiz.* vol. 2, pp. 836, 1959.

[4] K. R. Chu and J. L. Hirshfield, "Comparative study of the axial and azimuthal bunching mechanisms in electromagnetic cyclotron instabilities," *Phys. Fluids.* vol. 21, pp. 461–466, 1978.

[5] V. A. Flyagin, A. V. Gaponov, M. I. Petelin and V. K. Yulpatov, "The gyrotron," *IEEE Trans. Microwave Theory Tech.*, vol. MTT-25, pp. 514–521, 1977.

[6] J. L. Hirshfield and V. L. Granatstein, "The electron cyclotron maser—An historical survey," *IEEE Trans. Microwave Theory Tech.*, vol. MTT-25, pp. 522–527, 1977.

[7] A. A. Andronov, V. A. Flyagin, A. V. Gaponov, A. L. Gol'denburg, M. I. Petelin, V. G. Usov, V. K. Yulpatov, "The gyrotron; High power source of millimeter and submillimeter waves," *Infrared Phys.* vol. 18, pp. 385–394, Dec. 1978.

[8] V. L. Granatstein, P. Sprangle, M. Herndon, R. K. Parker, and S. P. Schlesinger, "Microwave amplification with an intense relativistic electron beam," J. *App. Phys.*, vol. 46, pp. 3800–3805, Sept, 1975.

[9] E. Ott and W. M. Manheimer, "Theory of microwave emission by velocity-space instabilities of an intense relativistic electron beam," *IEEE Trans. Plasma Sci.* vol. PS-3, pp. 1–5, 1975.

[10] H. S. Uhm, R. C. Davidson, and K. R. Chu, "Self-consistent theory of cyclotron maser instability for intense hollow electron beams," *Phys. Fluids*, vol. 21, pp. 1866–1876, 1978; and also pp. 1877–1886, 1978.

[11] B. Etlicher, A. Huetz, J. M. Buzzi, P. Haldenwand, and D. Lequeau, to be published.

[12] P. Sprangle and W. M. Manheimer, "Coherent nonlinear theory of a cyclotron instability," *Phys. Fluids.* vol. 18, pp. 224–230, 1975.

[13] P. Sprangle and A. T. Drobot, "The linear and self-consistent nonlinear theory of the electron cyclotron maser instability," *IEEE Trans. Microwave Theory Tech.*, vol. MTT-25, 528–544, 1977.

[14] K. R. Chu, A. T. Drobot, V. L. Granatstein, and J. L. Seftor, "Characteristics and optimum operating parameters of a gyrotron travelling wave amplifier," *IEEE Trans. Microwave Theory Tech.*, vol. MTT-27, pp. 178–187, 1979.

[15] S. Ahn and J. Y. Choe, *Bull. Amer. Phys. Soc.*, vol. 23, pp. 749, 1978.

[16] K. R. Chu and A. T. Drobot, "Theory and single wave simulation of the gyrotron travelling wave amplifier operating at cyclotron harmonics," Naval Research Lab., Washington, DC, Memo Rep. 3788 (unpublished).

[17] L. R. Barnett, K. R. Chu, J. Mark Baird, V. L. Granatstein, and A. T. Drobot, "Gain, saturation, and bandwidth measurements of the NR1 gyrotron travelling wave amplifier," *IEDM Tech. Dig.*, pp. 164–167, Dec. 1979..

[18] R. S. Symons, H. R. Jory, and S. J. Hogji, "An experimental gyro-TWT," *IEDM Tech. Dig.*, p. 676, Dec. 1979.